The Cryosphere Discuss., https://doi.org/10.5194/tc-2017-134
Manuscript under review for journal The Cryosphere
Discussion started: 14 August 2017


The Cryosphere Discussions
Open Access
EGU

# Crustal heat production and estimate of terrestrial heat flow in central East Antarctica, with implications for thermal input to the East Antarctic ice sheet

John W. Goodge[1]

[1]Department of Earth and Environmental Sciences, University of Minnesota, Duluth, MN 55812 USA

*Correspondence to*: John Goodge (jgoodge@d.umn.edu)

**Abstract.** Terrestrial heat flow is a critical first-order factor governing the thermal condition and, therefore, mechanical stability of Antarctic ice sheets, yet heat flow across Antarctica is poorly known. Previous estimates of terrestrial heat flow come from inversion of seismic and magnetic geophysical data, by modeling temperature profiles in ice boreholes, and by calculation from heat production values reported for exposed bedrock. Although accurate estimates of surface heat flow are important as an input parameter for ice-sheet growth and stability models, there are no direct measurements of terrestrial heat flow in East Antarctica coupled to either subglacial sediment or bedrock. Bedrock outcrop is limited to coastal margins and rare inland exposures, yet valuable estimates of heat flow in central East Antarctica can be extrapolated from heat production determined by the geochemical composition of glacial rock clasts eroded from the continental interior. In this study, U, Th and K concentrations in a suite of Proterozoic (1.2-2.0 Ga) granitoids sourced within the Byrd and Nimrod glacial drainages of central East Antarctica indicate average upper crustal heat production ($H_o$) of about 2.6 ± 1.9 μW m$^{-3}$. Assuming typical mantle and lower crustal heat flux for stable continental shields, and a length scale for the distribution of heat production in the upper crust, the heat production values determined for individual samples yield estimates of surface heat flow ($q_o$) ranging from 33-84 mW m$^{-2}$ and an average of 48.0 ± 13.6 mW m$^{-2}$. Estimates of heat production obtained for this suite of glacially-sourced granitoids therefore indicate that the interior of the East Antarctic ice sheet is underlain in part by Proterozoic continental lithosphere with average surface heat flow, providing constraints on both geodynamic history and ice-sheet stability. The ages and geothermal characteristics of the granites indicate that crust in central East Antarctica resembles that in the Proterozoic Arunta and Tenant Creek inliers of Australia, but is dissimilar to other areas characterized by anomalously high heat flow in the Central Australian Heat Flow Province. Age variation within the sample suite indicates that central East Antarctic lithosphere is heterogeneous, yet the average heat production and heat flow of four age subgroups cluster around the group mean, indicating minor variation in thermal contribution to the overlying ice sheet from upper crustal heat production. Despite their minor differences, ice-sheet models may favor a geologically realistic model of crustal heat flow represented by such a distribution of ages and geothermal characteristics.

The Cryosphere Discuss., https://doi.org/10.5194/tc-2017-134
Manuscript under review for journal The Cryosphere
Discussion started: 14 August 2017




## 1 Introduction

Heat production and heat flow are fundamental characteristics of continental crust (Rudnick and Fountain, 1995). Together they provide important constraints on the thermal and petrogenetic history of cratonic lithosphere, and heat flow is an indicator of modern geodynamic environments. Antarctic lithosphere is uniquely important because it underlies Earth's largest ice caps, including numerous subglacial lakes, and it is critical in governing the thermal state and mechanical stability of overlying ice (Pollard et al., 2005; Jamieson and Sugden, 2008; Van Liefferinge and Pattyn, 2013; Schroeder et al., 2014). Terrestrial heat flow in Antarctica has a strong influence on basal ice temperatures, amount of basal ice at its pressure melting point, and the formation of liquid water, all of which affect basal ice conditions, mechanical properties of glacial bed material, degree of basal sliding, erosional effectiveness, and the distribution of hydrologic networks and subglacial lakes (e.g., Siegert, 2000; Pollard et al., 2005; Pollard and DeConto, 2009). Despite its importance in governing ice-sheet mass balance—and therefore as an input parameter for ice-sheet growth and stability models—only a few estimates of conductive heat flow are available from temperature profiles in Antarctic ice (e.g., Fischer et al., 2013) and none from direct subglacial measurement. This is particularly problematic for East Antarctica, where the ice cap exceeds 4 km in many areas. In order to develop accurate models of past ice-sheet behavior and forward models of ice-sheet stability, it is therefore crucial to have good estimates of terrestrial heat flow from East Antarctica.

Continent-wide models for terrestrial heat flow come from both seismological and satellite magnetic data. To address a lack of direct heat flow measurements in Antarctica, Shapiro and Ritzwoller (2004) modeled surface heat flow by first correlating seismic velocity data from crust and upper mantle in regions of known heat flow, and then extrapolating these results to a seismic model of Antarctic lithosphere. Over a broad region of East Antarctica they estimated surface heat flow to be notably low, uniform, and similar to other old cratons (mostly 35-60 mW $m^{-2}$). Similarly, Fox Maule et al. (2005) used satellite magnetic data to model the depth to Curie temperature, and then inverted the resulting thermal profile to generate a distribution of heat flow (see also Purucker, 2012); this modeling likewise predicted heat flow in East Antarctica to be similar to the results obtained from seismology. In order to evaluate areas that may preserve very old ice, generally requiring thick, slow-moving ice under cold conditions with low basal heat flux, Van Liefferinge and Pattyn (2013) derived an average distribution of heat flow from a simple mean of existing geophysical models (Fig. 1); this continent-wide synopsis highlights a relatively uniform pattern of low heat flow in East Antarctica (mostly <55 mW $m^{-2}$). Using a thermal model that assumes basal ice temperatures above Antarctic subglacial lakes are equal to the pressure-melting value, Siegert (2000) estimated geothermal heat flow to vary between 37 and 65 mW $m^{-2}$, although most estimates for East Antarctica are <60 mW $m^{-2}$. In general terms, these different models, despite coarse kernel size, are consistent with one another and indicate heat flow in most of East Antarctica between about 35-60 mW $m^{-2}$.

In addition to models based on remote geophysical observations, there are also some field-based estimates. Using a measured temperature profile in the EPICA ice borehole at Dome C, Fischer et al. (2013) derived a geothermal heat flux of about 54 mW $m^{-2}$ by fitting a model of heat flow and basal ice melting to the thermal profile. A geological approach was

The Cryosphere Discuss., https://doi.org/10.5194/tc-2017-134
Manuscript under review for journal The Cryosphere
Discussion started: 14 August 2017




taken by Carson et al. (2014), who modeled heat flow using values for heat production estimated from the abundances of radioactive elements in crustal rocks sampled from outcrop near the Amery Ice Shelf (compiled by Carson and Pittard, 2012). From a coastal transect across rock exposures at Prydz Bay, the resulting profile indicates that heat flow in this area of Archean to Proterozoic igneous and metamorphic crust is highly variable over a distance of about 200 km, ranging from an average of 31 mW $m^{-2}$ in the Vestfold Hills, to 44 mW $m^{-2}$ in the Rauer Islands, and 55-70 mW $m^{-2}$ in the area of southern Prydz Bay. Locally, high heat-producing Cambrian granitoids indicate heat flow values as high as ~85 mW $m^{-2}$. Their model results thus show variable heat flow governed to first order by the age and type of crust represented, and punctuated by heat production spikes contributed from Th-rich granitoids. Although much of the area underlying the Rauer Islands and Vestfold Hills have low heat flow (<50 mW $m^{-2}$) typical of Proterozoic and Archean crust, Carson et al. (2014) emphasized that some early Paleozoic granites with anomalously high heat production can cause local elevation of heat flow (>80 mW $m^{-2}$), as observed in the Central Australian Heat Flow Province (McLaren et al., 2003). Thus, spatially coarse models of heat flow based on geophysical data across East Antarctica indicate relatively typical continental values ranging from about 35-60 mW $m^{-2}$, yet there are some indications of locally elevated heat flow in areas underlain by high heat-producing granites.

Although there are no measurements of terrestrial heat flow obtained directly from subglacial sediment or rock in East Antarctica, rock clasts eroded from the continental interior and transported to the margin can provide insight into the subglacial geology and, therefore, heat production. In this paper, the concentrations of heat-producing elements in glacial igneous rock clasts provide a unique opportunity to assess heat flow in the deep continental interior. The major ice drainages in East Antarctica are marked by nearly radial flow away from central ice divides and domes toward the continental margin (Fig. 2), providing natural proxy samples of the continental interior by bedrock erosion during glacial flow (Peucat et al., 2002; Goodge et al., 2008, 2010, 2017). Unique among the major drainages, glacial ice in Byrd Glacier and related smaller drainages moves non-radially from the main ice divides because it is obstructed by the high-standing Transantarctic Mountains (peak elevations >4000 m). Ice flows through the mountains via channelized outlet glaciers, but it also ablates in areas where it ramps up against the mountain range (Whillans and Cassidy, 1983). Glacial moraines are formed both along the margins of the outlet glaciers and where ice is ablating, forming lag deposits adjacent to the mountains. As part of a study of East Antarctic crustal history, glacial moraines were sampled at sites between the Byrd and Beardmore glaciers (Fig. 2). Ice-velocity fields show that material transported in the greater Byrd system may have been eroded from a broad area of central East Antarctica, potentially from near the upstream boundary along the major ice divide connecting Dome A and Dome C.

As proxies for subglacial geology, igneous clasts eroded from central East Antarctica and collected from moraines adjacent to the central Transantarctic Mountains were dated and analyzed geochemically for major and trace elements—including the major heat-producing elements U, Th and K—yielding values of radioactive heat production. Surface heat flow was then estimated by assuming mantle and lower crustal heat-flux contributions and a length scale for reduction in upper-crustal radiogenic heat production. The results indicate that heat production among most of the samples in this group is within the range expected for average continental crust and that terrestrial heat flow for a large region of central East

The Cryosphere Discuss., https://doi.org/10.5194/tc-2017-134
Manuscript under review for journal The Cryosphere
Discussion started: 14 August 2017




Antarctica is like that commonly observed in Precambrian shield areas. Estimates from this analysis corroborate previous models of heat flow in East Antarctica and can be used as first-order constraints in ice-sheet and lithospheric thermal models.

## 2 Glacial igneous clasts

Igneous rock samples were collected at five sites—Argo Glacier, Lonewolf Nunataks, Milan Ridge, Mt. Sirius, and Turret Nunatak—that yielded pre-Ross Orogen crystallization ages (>600 Ma), thereby providing evidence regarding composition and age of the Precambrian East Antarctic shield (Fig. 2). At Lonewolf Nunataks, elongate bands of distributed moraine and ice-matrix debris follow narrow flow lines related to ice movement along the southern margin of Byrd Glacier. Sites at Milan Ridge and Argo Glacier, directly adjacent to exposed Precambrian basement in the Miller Range, comprise thin, distributed morainal deposits dominated by a rich variety of crystalline rock types. Sites at Turret Nunatak and Mt. Sirius are dominated by Gondwanide debris, but they also yielded a small number of distinctive crystalline clasts. Together, these sites yielded a suite of pre-Ross igneous samples that were analyzed for their geochemical composition, age, and isotopic composition. The igneous clasts consist mainly of intermediate to felsic igneous rocks that represent magmatic components of the ice-covered East Antarctic craton (Goodge et al., 2017). They are granitic to granodioritic in composition and contain hornblende, biotite and/or muscovite; some samples are two-mica granitoids of peraluminous composition.

Zircon U-Pb ages from this suite of glacially-transported granitoid clasts show that the crust in central East Antarctica was formed by a series of magmatic events at ~2.01, 1.88-1.85, ~1.79, ~1.57, 1.50-1.41, and 1.20-1.06 Ga (Goodge et al., 2008, 2010, 2012, 2017). The dominant granitoid populations are ca. 1.85, 1.45 and 1.20-1.06 Ga. None of these igneous ages are known from the limited outcrop in the region. Samples of metamorphic rock clasts from the same moraines have similar Proterozoic ages ranging from about 1.1-1.9 Ga (Goodge et al., 2010; Nissen et al., 2013). By comparison with nearby mountain outcrops, the types and ages of these samples indicate that the crust of central East Antarctica comprises plutonic and metamorphic rocks unlike those seen in the central Transantarctic Mountains (Nimrod Complex ages of ca. 3.1, 2.5, and 1.7 Ga; Goodge et al. (2001); Goodge and Fanning (2016)). Likewise, they are different from igneous and metamorphic rocks exposed at the Terre Adélie coast (ages of ca. 2.4 and 1.7 Ga; Oliver and Fanning (1997)), although one population is similar in age to ~1.6 Ga glacial clasts sampled by Peucat et al. (2002). As shown in Figure 2, the glacially-eroded igneous clasts discussed here may also sample the Gamburtsev Subglacial Mountains, which is thought to have nucleated growth of the East Antarctic Ice Sheet (DeConto and Pollard, 2003; Bo et al., 2009; Rose et al., 2013).

## 3 Analytical methods

Bulk-rock X-ray fluorescence (XRF) and inductively-coupled plasma mass spectrometry (ICPMS) analyses of major and trace element compositions were completed in the GeoAnalytical Lab at Washington State University (Goodge et al., 2017). Prior to analysis, fresh chips of each sample were hand-picked and a standard amount (approximately 28 g) was ground in a swing mill with tungsten carbide surfaces for 2 minutes. For XRF analysis of major elements, 3.5 g of sample

powder was weighed into a plastic mixing jar with 7 g of spec pure dilithium tetraborate ($Li_2B_4O_7$). The mixed powders were emptied into graphite crucibles and loaded into a muffle furnace for fusion at 1000 °C. After removing from the oven to cool, each bead was reground in the swing mill and the resulting glass powders were replaced in the graphite crucibles and refused for 5 minutes, then cooled to form a glass bead. Their lower flat surfaces were then ground on 600 silicon carbide grit and finished briefly on a glass plate to remove any metal from the grinding wheel. The concentrations of 29 elements in the unknown samples were measured on a ThermoARL Advant'XP+ sequential X-ray fluorescence spectrometer by comparing the X-ray intensity for each element with the intensity obtained from USGS standard samples (PCC-1, BCR-1, BIR-1, DNC-1, W-2, AGV-1, GSP-1, G-2, and STM-1, using the values recommended by Govindaraju (1994) and beads of pure vein quartz used as blanks for all elements except Si. Twenty standard beads are routinely run and used for recalibration approximately once every three weeks or after the analysis of about 300 unknowns. The intensities for all elements were corrected for line interference and absorption effects due to all the other elements using the fundamental parameter method.

For trace elements, powdered samples were mixed with 2 g of $Li_2B_4O_7$ flux, placed in a carbon crucible and fused at 1000 °C in a muffle furnace for 30 minutes. After cooling, the resultant fusion bead was briefly ground in a carbon-steel ring mill and a 250 mg portion was weighed into a 30 ml, screw-top Teflon PFA vial for dissolution in water, $HNO_3$, $H_2O_2$, and HF and warmed on a hot plate until a clear solution was obtained. Samples were then diluted to a final weight of 60 g with de-ionized water. Solutions were analyzed for 27 elements on an Agilent model 4500 ICPMS and were diluted an additional 10x at the time of analysis using Agilent's Integrated Sample Introduction System (ISIS). This yielded a final dilution factor of 1:4800 relative to the amount of sample fused. Instrumental drift was corrected using Ru, In, and Re as internal standards, and applying a linear interpolation between In and Re to compensate for mass-dependent differences in the rate and degree of instrumental drift. Isobaric interferences of rare-earth and other oxides were optimized with correction factors using mixed-element solutions. Standardization was accomplished by analyzing duplicates of three in-house rock standards interspersed within each batch of 18 unknowns.

## 4 Heat production and estimated heat flow

### 4.1 Sample geochemical characteristics

Major, trace and rare-earth element geochemical data show that the granitoid samples are Si-rich and have >65 wt% $SiO_2$, and many have $SiO_2$ = 70-75 wt%. Trace-element compositions show that the samples have enriched light rare-earth element (LREE) and depleted heavy rare-earth element (HREE) abundances relative to chondrites, and they are enriched in large ion lithophile (LIL) elements and slightly depleted in high field-strength (HFS) elements relative to mid-ocean ridge basalt (MORB). Their trace and rare-earth element signatures are quite similar to modern continental-margin magmatic arc systems (e.g., Cascades, Andes) or evolved volcanic arcs, and they show very similar patterns and abundances as magmas interacting with thick crust (e.g., Davidson et al., 1990, 1991; Wörner et al., 1994). Some of the samples resemble Si-rich, peraluminous leucogranites found in regions of over-thickened continental crust (Frost et al., 2001). In broad terms, then, the



trace-element compositions indicate that the melts that produced these igneous rocks interacted with thick, evolved continental crust, but that they are dissimilar generally from intraplate granitoids.

### 4.2 Heat-producing elements

The concentrations of the heat-producing elements U, Th and K in 18 granitoid samples are listed in Table 1. The concentration of U is generally low, ranging up to about 6 ppm (mean = 2.0). Thorium ranges widely, from 1-98 ppm (mean = 23.7), and K similarly varies from 0.5-8 wt% $K_2O$ (mean = 4.34).

### 4.3 Heat production

The geochemical compositions of igneous rocks can be used to determine crustal heat production based on their concentrations of radioactive elements. Heat production ($H_o$) was calculated for these clast samples based on rock density and concentrations of U, Th and K by applying two different algorithms:

$$H_o = 10^{-2} * \rho * (9.67CU + 2.63CTh + 3.48CK) \quad (1)$$

$$H_o = \rho * 0.9928CU*H(^{238}U) + 0.0071CU*H(^{235}U) + CTh*H(Th) + 1.19x10^{-4}CK^{40}*H(^{40}K) \quad (2)$$

where $H_o$ is surface heat production ($\mu W\ m^{-3}$), $\rho$ is density ($kg\ m^{-3}$), CU is the concentration of U (ppm), CTh is the concentration of Th (ppm), CK is the concentration of $K_2O$ (wt%), $H(^{238}U)$ is the heat production from the isotope $^{238}U$ ($9.37x10^{-5}$ W $kg^{-1}$), $H(^{235}U)$ is the heat production from the isotope $^{235}U$ ($5.69x10^{-4}$ W $kg^{-1}$), H(Th) is the heat production from the isotope $^{232}Th$ ($2.69x10^{-5}$ W $kg^{-1}$), and $H(^{40}K)$ is the heat production from the isotope $^{40}K$ ($2.79x10^{-5}$ W $kg^{-1}$). Method 1 was calculated from the formula of Rybach (1976, 1988), using values from Hasterok and Chapman (2011). Method 2 uses the formulation of Turcotte and Schubert (2014). Density ($\rho$) was assumed to be $2.7 \times 10^3$ kg $m^{-3}$ in all cases. Using Method 1, the igneous clast compositions yield estimates of heat production ranging from 0.25-7.49 $\mu W\ m^{-3}$, with an average of about 2.6 $\mu W\ m^{-3}$ and 1σ standard deviation of 1.9 $\mu W\ m^{-3}$ (Table 1). Most of the variation observed in these samples comes from variations in concentrations of U and Th. Method 2 gives quite similar results.

Estimates of heat production versus age are plotted in Fig. 3. Compared to an average value for surface heat production in stable continental shield regions of ~2 $\mu W\ m^{-3}$ (Jaupart et al., 2016), most of the Antarctic clast samples are of similar magnitude (mean of 2.61 $\mu W\ m^{-3}$, with 11 falling between 1-4 $\mu W\ m^{-3}$), although they are notably higher than values reported for some cratonic areas (e.g., Canadian Shield and Grenville Orogen; Mareschal and Jaupart, 2013; Jaupart et al., 2016). As a group, they are quite similar to the global average granitic heat production of 2.5 $\mu W\ m^{-3}$ (Rybach, 1976; Haenel et al., 1988), which in general is expected to be higher than the bulk upper crustal average of about 1.6 $\mu W\ m^{-3}$ (Jaupart et al., 2016). Heat production from the clasts is comparable to estimates obtained from Archean and Paleoproterozoic bedrock exposed in the coastal region of southern Prydz Bay (2.4-2.6 $\mu W\ m^{-3}$; Carson and Pittard, 2012; Carson et al., 2013). Four of the clasts give high values between 4.0-7.5 $\mu W\ m^{-3}$, which are similar to global occurrences of crust characterized by high

The Cryosphere Discuss., https://doi.org/10.5194/tc-2017-134
Manuscript under review for journal The Cryosphere
Discussion started: 14 August 2017




heat production (Mareschal and Jaupart, 2013; Jaupart et al., 2016) and exemplified by the Central Australian Heat Flow Province (CAHFP; Sandiford and McLaren, 2002; McLaren et al., 2003). Nonetheless, all but two of the samples in this suite have heat production less than the mean for the CAHFP (4.6 μW $m^{-3}$).

The variability in heat production shown by the data presented here resembles that observed in regions comprised by Precambrian shields or granitic batholiths and likely represents real heterogeneities in the source region. Although the precise distribution of heat-producing rocks in the source area from which these clast samples were eroded is not known, this group may collectively provide a qualitatively-random sample that provides a means to assess average heat production for a broad region of the continental interior. Compared to global examples, the Proterozoic igneous rocks in this study indicate that heat production in central East Antarctica is like that of typical continental shield areas and demonstrably different from the anomalously warm region represented by the CAHFP. Therefore, despite plausible geological and geophysical correlations between cratonic rocks in southern Australia (Gawler craton) and the Wilkes Land region of East Antarctica (e.g., Oliver and Fanning, 1997; Aitken et al., 2014; Goodge and Finn, 2010; Boger, 2011; Goodge and Fanning, 2016), extrapolation of the high values reported for the CAHFP into East Antarctica may be unwarranted.

### 4.4 Heat flow

Geothermal heat flow can be estimated from the empirical relation with crustal heat production (Lachenbruch, 1968; Roy et al., 1968). In the absence of direct terrestrial heat flow measurements, as is the case for Antarctica, it is possible to calculate heat flow from heat production by assuming a thickness of the upper crustal heat-producing layer (Sandiford and McLaren, 2002; Turcotte and Schubert, 2014). This thickness, $h_r$, is the length scale for decrease in $H_o$ with depth in the upper crust (where most heat-producing elements are concentrated) and is determined from the slope of the q-H function. Although $H_o$ is thought to decrease exponentially with depth (Lachenbruch, 1968), a first-order estimate of terrestrial heat flow can be obtained from:

$$q_o = q_m + q_r + (H_o * h_r) \quad (3)$$

where $q_o$ is the surface heat flow (mW $m^{-2}$), $q_m$ is the mantle heat flow, $q_r$ is the 'reduced' heat flow contributed by heat production in the middle and lower crust, and other terms are as defined above. For stable Precambrian continental crust, average values for $q_m$ are about 14 mW $m^{-2}$ and $q_r$ is about 15 mW $m^{-2}$ (Sandiford and McLaren, 2002; Perry et al., 2006; Levy et al., 2010; Mareschal and Jaupart, 2013; Jaupert et al., 2016). Based on similarities in age and thickness to the Canadian and Scandinavian shields, a value of 7.3 km for $h_r$ is used here. Using the relationship above and heat production results, the surface terrestrial heat flow is estimated from the igneous clast population to range from about 31-84 mW $m^{-2}$ (Table 1), with an average of 48.0 ± 13.6 mW $m^{-2}$ (1σ standard deviation; Fig. 4). The average value may be regarded as an integrated estimate of heat flow across the area of erosion within the catchment, but it is probably a maximum because it is derived from values of heat production that are biased to crustal granites.

The Cryosphere Discuss., https://doi.org/10.5194/tc-2017-134
Manuscript under review for journal The Cryosphere
Discussion started: 14 August 2017




### 4.5 Uncertainties

Because estimates of heat flow are used in ice-sheet models, it is important to consider uncertainties in the values used as input parameters. Here I consider uncertainties in the estimates of heat production and heat flow provided above.

#### 4.5.1 Uncertainties in $H_o$

Laboratory precision on elemental analyses is very high (instrumental precision within 0.2% for $K_2O$ by XRF and within 2% for U and Th by ICPMS), density is assumed, and constants of heat-production for various elements are assumed. Therefore, individual uncertainties for $H_o$ were not calculated because they are expected to be very low relative to other parameters involved in calculation of heat flow.

#### 4.5.2 Uncertainties in $q_o$

Uncertainties in the linear relationship used to calculate surface heat flow ($q_o$) can be modeled using the following expression:

$$\Delta q_o = \Delta q_m + \Delta q_r + (\overline{H}_o * \Delta h_r) + (\overline{h}_r * \Delta H_o) \quad (4)$$

where $\Delta q_o$ is the sum of uncertainties represented by the variables included in equation (3). Determining reasonable values for most of the $\Delta$ terms is problematical because the corresponding terms in the heat-flow equation are either based on model-derived values or are simply poorly constrained by limited empirical data. Because geological and seismological data indicate that East Antarctica is a stable craton, we can use typical cratonic values for $q_m$ and $q_r$ as a basis for evaluating uncertainty in these terms. For this analysis, $\Delta q_m$ is taken to be ±2.5 mW $m^{-2}$ based on a compilation of estimates worldwide for stable continental shield areas that range mostly from 12-17 mW $m^{-2}$ (Mareschal and Jaupart, 2013; Jaupart et al., 2016). Uncertainty in the lower-crustal term, $\Delta q_r$, is taken to be 3.0 mW $m^{-2}$, assumed as a general variance (±20%) around a representative value of 15 mW $m^{-2}$ for lower-crustal heat flow. A mean value of $\overline{H}_o$ = 2.6 μW $m^{-3}$ is used from the data reported here and the representative average value of $\overline{h}_r$ = 7.3 km that was used to calculate heat flow is assumed here. Uncertainty in heat production, $\Delta H_o$, is taken as a 1σ standard deviation of the calculated values (1.86 mW $m^{-2}$), and uncertainty in the length scale, $\Delta h_r$, is assumed to be 1500 m (±20%). Based on these inputs, we can derive a general uncertainty for the surface heat flow term ($\Delta q_o$) of about 23 mW $m^{-2}$ (Fig. 4). This is a large value compared to the nominal mean value of 48 mW $m^{-2}$ obtained here, and it reflects large natural variability in lithosphere properties as well as few direct constraints on mantle heat flow, lower crustal heat flow, and the vertical distribution of heat-producing elements in continental crust. Of this estimated uncertainty, 24% is contributed by the $\Delta q_m$ and $\Delta q_r$ terms, and 76% is attributed to the multiplying effects of the thickness and uncertainty of the upper-crustal heat-producing layer ($\overline{h}_r$ and $\Delta h_r$). Only 8% is contributed by $\Delta H_o$ itself. Together, the large combined uncertainty is therefore contributed mainly by mantle heat flow, lower crustal heat flow, and the vertical distribution of heat-producing elements; conversely, estimates of upper crustal heat

The Cryosphere Discuss., https://doi.org/10.5194/tc-2017-134
Manuscript under review for journal The Cryosphere
Discussion started: 14 August 2017




production from the glacial clast samples are not an important source of uncertainty. Nonetheless, the overall range in surface heat flow covered by this uncertainty is consistent with the range of values reported for other cratons, lending support to the idea that the recovered glacial clasts are indeed representative of heat flow known from typical Archean and Proterozoic shield areas. Despite the inherent large uncertainties, the first-order results can help to inform future ice-sheet modeling.

## 5 Discussion

The glacial igneous clasts sampled for this study indicate that upper crustal heat production for at least a part of central East Antarctica is in the range of 0.3-7.5 μW $m^{-3}$, with average value of 2.6 ± 1.9 μW $m^{-3}$. Assuming typical values of mantle heat flux, lower-crustal heat flux, and an upper-crustal length factor appropriate for stable continental cratons, the derived heat production corresponds to an average surface heat flux of 48 mW $m^{-2}$. Although this approach assumes cratonic values for mantle and lower-crustal contributions, it is reasonable given what is known about East Antarctic lithosphere. The net upper crustal contribution to surface heat flow is therefore about 19 mW $m^{-2}$. The total surface heat flux is quite similar to the average heat flux of 53 mW $m^{-2}$ from 13 cratonic shield provinces globally (Jaupart et al., 2016). Likewise, Nyblade and Pollack (1993) found average surface heat flow values of 42 mW $m^{-2}$ for Archean provinces and 47 mW $m^{-2}$ for Paleoproterozoic provinces, which represents a general depletion of heat-producing elements in continental crust with increasing age. The heat flow results obtained here are also similar to earlier estimates for East Antarctica determined by geophysical modeling and inversion of ice borehole temperature profiles, which indicate a broad region with low to moderate values of 50-60 mW $m^{-2}$.

Taken together, the heat production and surface heat flow values estimated for the glacial igneous clasts discussed here appear to be representative of typical Archean-Proterozoic cratonic lithosphere. As a group they are distinctly different from the regional pattern shown by anomalously warm Proterozoic crust in central Australia with average $q_o$ = 80 mW $m^{-2}$ (McLaren et al., 2003), which has been suggested to extend across the Wilkes Land margin of Antarctica based on Gondwana supercontinent reconstructions (Carson et al., 2014; Aitken et al., 2014). Despite general age similarities among some of the clast population with parts of the Gawler Craton, and basement age correlations that indicate continuity of Mawson-type crust into the Wilkes sector of East Antarctica (Goodge and Fanning, 2016), the proxy heat production determinations and heat flow estimates provided here suggest that central portions of the East Antarctic ice sheet are underlain by stable continental crust with quite normal thermal properties represented by average values of heat production of about 2.5 μW $m^{-3}$ and heat flow of about 50 mW $m^{-2}$.

Estimates of terrestrial heat flow such as those provided here can also be used to assess the effect of heat flow on ice-sheet mass balance. For example, Pollard et al. (2005) evaluated the effect of varying heat flow regimes on ice-sheet behavior by modeling changes in Antarctic ice volume, ice-sheet surface elevation, and area of the base at its pressure-melting point as a function of differing heat-flow regimes. Their models used three different geothermal heat flow

The Cryosphere Discuss., https://doi.org/10.5194/tc-2017-134
Manuscript under review for journal The Cryosphere
Discussion started: 14 August 2017




distributions: (a) uniform heat flow of 37.7 mW $m^{-2}$, representing typical values of Archean cratons; (b) uniform at 75.4 mW $m^{-2}$, to mimic Proterozoic lithosphere characterized by high crustal heat production; and (c) spatially varying heat flow based on the distributions of different crustal provinces extrapolated from craton-margin geology, and including values of 41 and 55 mW $m^{-2}$ across most of East Antarctica. The values of heat production and heat flow estimated for central East Antarctica in this study are most consistent with their third approach; the average heat flow value of the Proterozoic granitoid samples is higher than in the case of uniform Archean lithosphere, yet lower than that assumed for Proterozoic lithosphere with high crustal heat production. Because the modeling of Pollard et al. (2005) shows a large effect of heat flow on the area of the ice-sheet base at its pressure-melting point, inputting appropriate values of crustal heat flow is vitally important for predicting, for example, the thermal and physical conditions of the basal ice-sheet regime.

To provide a simple model for the distribution of heat flow across the catchment area sampled in this study, mean heat flow values were calculated in two ways (Table 2). First, the set of 18 samples was divided into equal quintiles representing ranges of 10 mW $m^{-2}$ each. Average heat flow values were calculated for each quintile, as was a percentage of the measurements falling in that range (Fig. 5a). Each quintile thus represents a proportionally-based average heat flow value that could be used as an input for ice sheet models. Assuming that the igneous and metamorphic crust beneath the EAIS is heterogeneous in age and composition, this proportional distribution of heat flow values may better reflect the complexities of crustal geothermal input as a function of subglacial area compared to a simple average. Second, the samples were grouped by age and average heat flow values calculated for each of four groups (Fig. 5b). This approach provides a reasonable estimate of heat flow potentially contributed by igneous crust proportionally represented by different age groups. Although the sample values were divided arbitrarily into five groups using the first method, this approach shows that about 61% of the sample results are <50 mW $m^{-2}$ (also indicated by the skewed distribution of values in Figure 4), indicating that the bulk of crust underlying the EAIS has relatively low long-range average heat flow. The second approach, perhaps more useful from a modeling perspective because it groups samples by age, illustrates that for individual age groups the values are also quite modest, ranging from about 42-55 mW $m^{-2}$ and similar to the total group average. It is noteworthy that this range is nearly identical to the heterogeneous heat-flow model adopted by Pollard et al. (2005), appearing to validate the earlier study. Future ice-sheet stability modeling combined with the estimates of low to intermediate sub-glacial heat flow found in this study may thus help to further refine predictions of ice-sheet behavior.

## 6 Conclusions

Based on geochemical analysis of a suite of glacially-eroded granitic rock clasts, average heat production from an inferred large Proterozoic igneous crustal province in central East Antarctica is estimated to be about 2.5 μW $m^{-3}$, and the corresponding average surface heat flow is about 48 mW $m^{-2}$. These geothermal properties are quite similar to average Archean and Proterozoic cratonic shields globally, despite being biased here to granitic compositions. Although the source of the granite clasts is not precisely known, they were likely derived from a region extending into central East Antarctica from



near the inlet to Byrd Glacier. This region contrasts with other areas marked by high heat flow, such as the Central Australia Heat Flow Province and some parts of East Antarctica near Prydz Bay, indicating that crust in those areas does not extend into central regions of the continental interior.

Heat flow estimated in this study is valuable for several reasons. First, the values are very similar to an estimate of heat flow derived by modeling of a borehole temperature profile near Dome C (54 mW $m^{-2}$; Fischer et al., 2013), helping to validate the earlier model finding. Likewise, they are consistent with the general range of values indicated by inversion of geophysical data from cratonic East Antarctica (e.g., Shapiro and Ritzwoller, 2004; Fox Maule et al., 2005). In detail, the values obtained here show a similar range to those indicated in the model derived from magnetic data (Fox Maule et al., 2005), both of which indicate that lithologic and, therefore, geothermal variations are real. Second, the new data provide a unique estimate of heat production and terrestrial heat flow that can be used as an input to ice-sheet stability models. In particular, they validate the general approach by Pollard et al. (2005) in which basal heat flow is varied by area depending on age and character of the subglacial geology. There is similar variability within this sample group that probably reflects the lithologic heterogeneity to be expected in continental shields. Third, although the data presented here provide a good approximation of both heat production and heat flow in an otherwise inaccessible region of East Antarctica, the existing uncertainties associated with extrapolating heat flow from heat production illustrate the critical need for precise *in-situ* measurement of terrestrial heat flow from the subglacial environment. One attempt to do so beneath the Whillans Ice Stream in West Antarctica (Fisher et al., 2015) measured a heat flux of 285 mW $m^{-2}$. This extraordinarily high value, even greater than that observed on modern ocean ridges (typically ~100-250 mW $m^{-2}$ near the ridge axis and one third of that for oceanic crust >50 Ma; Stein, 1995), likely reflects a large component of advective heat transport by flowing water and is therefore not representative of terrestrial heat flow in West Antarctica. Despite the difficulty in obtaining reliable heat flow data from the subglacial environment, it should be a high research priority that can be addressed by drilling through the ice sheets at as many sites as possible in order to assess crustal heterogeneity. Last, these estimates of low to moderate crustal heat flow indicate that some large regions of the interior East Antarctic ice sheet may be expected to be frozen at the bed, which is of use to future drilling projects that plan to intersect the glacial bed.

**Data availability.** Data supporting the conclusions are listed in Table 1.

**Sample availability.** Samples referred to in this study are housed at the University of Minnesota Duluth and available on request to the author.

**Competing interests.** The author declares that he has no conflict of interest.

**Acknowledgments.** Field and analytical portions of this project were supported by the National Science Foundation (award 0944645). Jacqueline Halpin and Jean-Claude Mareschal provided helpful feedback on the approach to estimating heat

production and heat flow, and Jeff Severinghaus kindly reviewed an earlier draft manuscript. John Swenson kindly provided insight into the treatment of uncertainties.

**References**

Aitken, A.R.A., Young, D.A., Ferraccioli, F., Betts, P.G., Greenbaum, J.S., Richter, T.G., Roberts, J.L., Blankenship, D.D., Siegert, M.J.: The subglacial geology of Wilkes Land, East Antarctica, Geophysical Research Letters, 41, doi:10.1002/2014GL059405, 2014.

Bo, S., Siegert, M.J., Mudd, S.M., Sugden, D., Fujita, S., Xiangbin, C., Yunyun, J., Xueyuan, T., Yuansheng, L.: The Gamburtsev Mountains and the origin and early evolution of the Antarctic Ice Sheet, Nature, 459, 690–693, doi:10.1038/nature08024, 2009.

Boger, S.D.: Antarctica — Before and after Gondwana, Gondwana Research, 19, 335-371, doi: 10.1016/j.gr.2010.09.003, 2011.

Carson, C.J., McLaren, S., Roberts, J.L., Boger, S.D., Blankenship, D.D.: Hot rocks in a cold place: high sub-glacial heat flow in East Antarctica, J. Geol. Soc. Lond., doi:10.1144/jgs2013-030, 2013.

Carson, C.J., Pittard, M.: A reconnaissance crustal heat production assessment of the Australian Antarctic Territory (AAT), Geoscience Australia Record, Report 2012-63, 2012.

Davidson, J.P., McMillan, N.J.M., Moorbath, S., Wörner, G., Harmon, R.S., López-Escobar, L.: The Nevados de Payachata volcanic region (18S/69W, N. Chile) II. Evidence for widespread crustal involvement in Andean magmatism, Contributions to Mineralogy and Petrology, 105, 412–432, 1990.

Davidson, J.P., Harmon, R.S., Wörner, G.: The source of central Andean magmas: Some considerations. In Harmon, R.S., and Rapela, C.W. (eds.), Andean Magmatism and Its Tectonic Setting, Geological Society of America Special Paper, 265, 233–244, 1991.

DeConto, R.M., Pollard, D.: Rapid Cenozoic glaciation of Antarctica induced by declining atmospheric $CO_2$, Nature, 421, 245–249, doi:10.1038 /nature01290, 2003.

Fischer, H., Severinghaus, J., Brook, E., and 27 others: Where to find 1.5 million yr old ice for the IPICS “Oldest-Ice” ice core, Clim. Past, 9, 2489-2505, doi:10.5194/cp-9-2489-2013, 2013.

Fisher, A.T., Mankoff, K.D., Tulaczyk, S.M., Tyler, S.W., Foley, N., and the WISSARD Science Team: High geothermal heat flux measured below the West Antarctic Ice Sheet, Science Advances, 1(6), 1-9, doi:10.1126/sciadv.1500093, 2015.

Fox Maule, C., Purucker, M.E., Olsen, N., Mosegaard, K.: Heat flux in Antarctica revealed from satellite magnetic data, Science, 309, 464-467, doi:10.1126/science.1106888, 2005.

Frost, B.R., Barnes, C.G., Collins, W.J., Arculus, R.J., Ellis D.J., Frost, C.D.: A geochemical classification for granitic rocks, J. Petrology, 42, 2033-2048, doi:10.1093/petrology/42.11.2033, 2001.

Goodge, J.W., Fanning, C.M., Bennett, V.C.: U-Pb evidence of ~1.7 Ga crustal tectonism during the Nimrod Orogeny in the Transantarctic Mountains, Antarctica: implications for Proterozoic plate reconstructions, Precambrian Research, 112, 261-288, doi:10.1016/S0301-9268(01)00193-0, 2001.

Goodge, J.W., Fanning, C.M., Brecke, D.M., Licht, K.J., Palmer, E.F.: Continuation of the Laurentian Grenville province in western East Antarctica, Journal of Geology, 118, 601-619, doi:10.1086/656385, 2010.

Goodge, J.W., Fanning, C.M., Vervoort, J.D., Radakovich, A.L.: More SWEAT: Discovery of Mesoproterozoic and Paleoproterozoic igneous crust in East Antarctica strengthens the case for Laurentia-Antarctica connections in Rodinia, Geological Society of America Abstracts with Programs, 44(7), 599, 2012.

Goodge, J.W., Vervoort, J.D., Fanning, C.M., Brecke, D.M., Farmer, G.L., Williams, I.S., Myrow, P.M., DePaolo, D.J.: A positive test of East Antarctica-Laurentia juxtaposition within the Rodinia supercontinent, Science, 321, 235-240; doi:10.1126/science.1159189, 2008.

Goodge, J.W., Fanning, C.M.: Mesoarchean and Paleoproterozoic history of the Nimrod Complex, central Transantarctic Mountains, Antarctica: Stratigraphic revisions and relation to the Mawson Continent in East Gondwana, Precambrian Research, 285, 242-271, doi:10.1016/j.precamres.2016.09.001, 2016.

Goodge, J.W., Fanning, C.M., Fisher, C.M., Vervoort, J.D.: Proterozoic crustal evolution of central East Antarctica: Age and isotopic evidence from glacial igneous clasts, and links with Australia and Laurentia, Precambrian Research, in press, 2017.

Govindaraju, K.: Compilation of working values and sample description for 383 geostandards, *Geostandards Newsletter*, 18 (Special Issue), 1-158, 1994.

Haenel, R., Rybach, L., Stegena L., eds.: Handbook of Terrestrial Heat-Flow Density Determination: Dordrecht, Kluwer Academic Publishers, 486 pp, 1988.

Hasterok, D., Chapman, D.S.: Heat production and geotherms for the continental lithosphere, Earth and Planetary Science Letters, 307, 59–70, doi: 10.1016/j.epsl.2011.04.034, 2011.

Jamieson, S.S.R., Sugden, D.E.: Landscape Evolution of Antarctica. In Cooper, A.K., Barrett, P.J., Stagg, H., Storey, B., Stump, E., Wise, W., eds., Antarctica: A Keystone in a Changing World (Proceedings of the 10th International Symposium on Antarctic Earth Sciences). Washington, DC, The National Academies Press, 2008.

Jaupart, C., Mareschal, J.-C., Iarotsky, L.: Radiogenic heat production in the continental crust, Lithos, 262, 398-427, 10.1016/j.lithos.2016.07.017, 2016.

Lachenbruch, A.H.: Preliminary geothermal model of the Sierra Nevada, Journal of Geophysical Research, 73, 6977–6989, 1968.

Lévy, F., Jaupart, C., Mareschal, J., Bienfait, G., Limare, A.: Low heat flux and large variations of lithospheric thickness in the Canadian Shield, Journal of Geophysical Research, 115, 6404, 2010.

Mareschal, J.-C., Jaupart, C.: Radiogenic heat production, thermal regime and evolution of continental crust, Tectonophysics, 609, 524–534, doi:10.1029/2009JB006470, 2013.

McLaren, S., Sandiford, M., Hand, M., Neumann, N., Wyborn, L., Bastrakova, I.: The hot southern continent: heat flow and heat production in Australian Proterozoic terranes. In Hillis, R.R., Müller, R.D. (eds.), Evolution and Dynamics of the Australian Plate, Geological Society of Australia Special Publications, 12(22), 151–161, 2003.

Nissen, C.I., Fanning, C.M., and Goodge, J.W.: New evidence of Proterozoic metamorphic events in East Antarctica from in-situ U-Pb age dating of monazite in metamorphic glacial clasts, central Transantarctic Mountains, Antarctica, Geological Society of America Abstracts with Programs, 45, 798, 2013.

Nyblade, A.A.: Heat flow and the structure of Precambrian lithosphere, Lithos, 48, 81–91, 1999.

Nyblade, A.A., Pollack, H.N.: A global analysis of heat flow from Precambrian terrains: implications for the thermal structure of Archean and Proterozoic lithosphere, Journal of Geophysical Research, 98, 12207–12218, 1993.

Oliver, R.L., Fanning, M.: Antarctica: precise correlation of Paleoproterozoic terrains, In Ricci C. A., ed., The Antarctic Region: Geological Evolution and Processes, Siena, Terra Antarctica Publications, 163–172, 1997.

Perry, H., Rosieanu, C., Mareschal, J.C., Jaupart, C.: Thermal regime of the lithosphere in Canada, Canadian Journal of Earth Sciences, 47, 389–408, doi:10.1139/E09-059, 2010.

Peucat, J.-J., Capdevila, R., Fanning, C.M., Ménot, R.-P., Pécora, L., Testut, L.: 1.60 Ga felsic volcanic blocks in the moraines of the Terre Adélie craton, Antarctica: Comparisons with the Gawler Range volcanics, South Australia, Australian Journal of Earth Sciences, 49, 831-845, doi:10.1046/ j.1440-0952.2002.00956, 2002.

Pollard, D., DeConto R.M., Nyblade, A.A.: Sensitivity of Cenozoic Antarctic ice sheet variations to geothermal heat flux, Glob. Planet. Change, 49, 63-74, doi:10.1016/j.gloplacha.2005.05.003, 2005.

Purucker, M.E.: Antarctica Basal Heat Flux, http://websrv.cs.umt.edu/isis/index.php/Antarctica_Basal_Heat_Flux, 2012.

Rignot, E., Mouginot, J., Scheuchl, B.: Ice flow of the Antarctic ice sheet, Science, 333, 1427-1430; doi:10.1126/science.1208336, 2011.

Rose, K.C., Ferraccioli, F., Jamieson, S.S.R., Bell, R.E., Corr, H., Creyts, T.T., Braaten, D., Jordan, T.A., Fretwell, P.T., Damaske, D.: Early East Antarctic Ice Sheet growth recorded in the landscape of the Gamburtsev Subglacial Mountains, Earth and Planetary Science Letters, 375, 1–12, doi:10.1016/j.epsl.2013 .03.053, 2013.

Roy, R.F., Blackwell, D.D., Birch, F.: Heat generation of plutonic rocks and continental heat flow provinces, Earth and Planetary Science Letters, 5, 1–12, 1968.

Rudnick, R.L., Fountain, D.M.: Nature and composition of the continental crust: a lower crustal perspective, Reviews of Geophysics, 33, 267–309, 1995.

Rybach, L.: Radioactive heat production in rocks and its relation to other petrophysical parameters, Pure and Applied Geophysics, 114, 309–317, 1976.

Rybach, L.: Determination of heat production rate, In R. Haenel, L. Rybach, L. Stegena, (eds.), Handbook of Terrestrial Heat-Flow Density Determination, Kluwer Academic Publishers, Dordrecht, pp. 125-142, 1988.

Sandiford, M., McLaren, S.: Tectonic feedback and the ordering of heat producing elements within the continental lithosphere, Earth and Planetary Science Letters, 204, 133–150, doi:10.1016/S0012-821X(02)00958-5, 2002.

Schroeder, D.M., Blankenship, D.D., Young, D.A., Quartini, E.: Evidence for elevated and spatially variable geothermal flux beneath the West Antarctic Ice Sheet, Proc. Natl. Acad. Sci. U. S. A., 111(25), 9070–9072, 2014.

Shapiro, N.M., Ritzwoller, M.H.: Inferring surface heat flux distributions guided by a global seismic model: particular application to Antarctica, Earth Planet. Sci. Lett., 223, 213–224, 2004.

Siegert, M.J.: Antarctic subglacial lakes, Earth-Science Reviews, 50, 29–50, 2000.

Stein, C.: Heat flow of the Earth, In Global Earth Physics: A Handbook of Physical Constants, American Geophysical Union, Washington, D.C., Reference Shelf 1, 144-158, 1995.

Turcotte, D.L., Schubert, G.: Geodynamics, Cambridge, Cambridge University Press, 623 p, 2014.

Van Liefferinge, B., Pattyn, F.: Using ice-flow models to evaluate potential sites of million year-old ice in Antarctica, Clim. Past, 9, 2859–2887, doi:10.5194/cpd-9-2859-2013, 2013.

Whillans, I.M., Cassidy, W.A.: Catch a falling star: Meteorites and old ice, Science, 222, 55-57, 1983.

Wörner, G., Moorbath, S., Horn, S., Entenmann, J., Harmon, R.S., Davidson, J., López-Escobar, L.: Large- and fine-scale geochemical variations along the Andean arc of northern Chile (17. 5–22S), In K.J. Reutter, E. Scheuber, and P.J. Wigger, eds., Tectonics of the Southern Central Andes: Structural Evolution of an Active Continental Margin, Springer-Verlag, Berlin, 77–92, 1994.

The Cryosphere Discuss., https://doi.org/10.5194/tc-2017-134
Manuscript under review for journal The Cryosphere
Discussion started: 14 August 2017


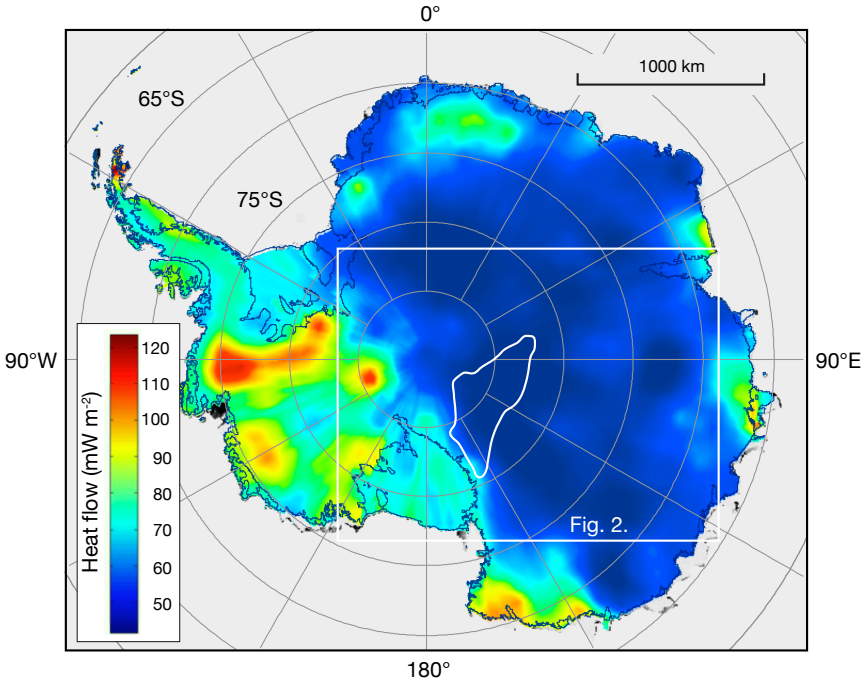


**Figure 1: Terrestrial heat flow in Antarctica, from the mean geothermal heat flux model of Van Liefferinge and Pattyn (2013), which averages heat flow determined from multiple geophysical datasets. Inset white box shows area of Figure 2, including glacial drainage sourcing bedrock igneous rock clasts (white outline).**

The Cryosphere Discuss., https://doi.org/10.5194/tc-2017-134
Manuscript under review for journal The Cryosphere
Discussion started: 14 August 2017


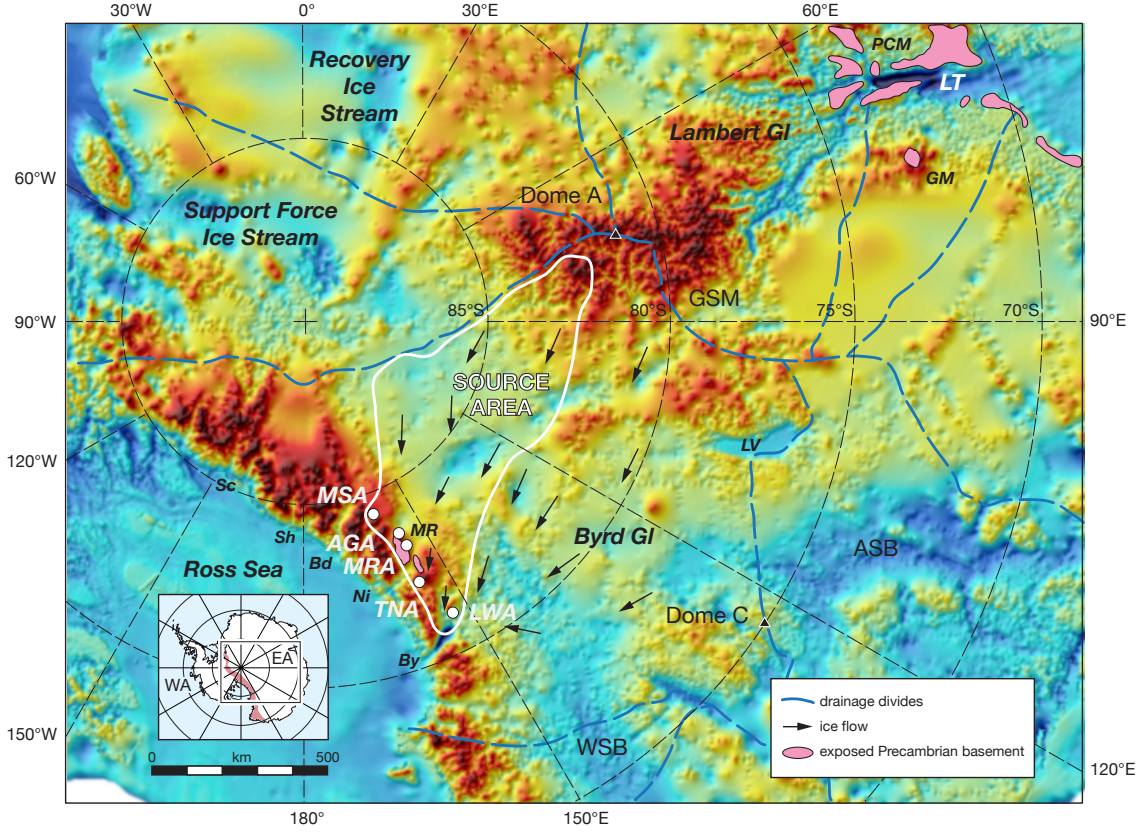


**Figure 2: Map showing potential source areas for dated glacial igneous clasts, superimposed on the Bedmap2 subglacial topography of East Antarctica (Fretwell et al., 2013). Principal features are ice-sheet catchment areas (marked by thin blue drainage divides), ice flow directions in the broad Byrd Glacier drainage (arrows, Rignot et al. (2011), and areas of Precambrian basement exposure (pink). Composite source area (outlined by heavy white line) was determined from the ice flow-fields that contribute ice to each of the five sample sites (white circles). Because transport distance is not known for any of the individual clasts, possible bedrock sources could lie anywhere between the sample sites and the top of the ice-shed overlapping the Gamburtsev Subglacial Mountains (GSM). Other abbreviations: ASB, Aurora Subglacial Basin; GM, Grove Mountains; LT, Lambert trough; LV, Lake Vostok; MR, Miller Range; PCM, Prince Charles Mountains; WSB, Wilkes Subglacial Basin. Outlet glaciers: Bd, Beardmore; By, Byrd; Ni, Nimrod; Sc, Scott; Sh, Shackleton.**

The Cryosphere Discuss., https://doi.org/10.5194/tc-2017-134
Manuscript under review for journal The Cryosphere
Discussion started: 14 August 2017


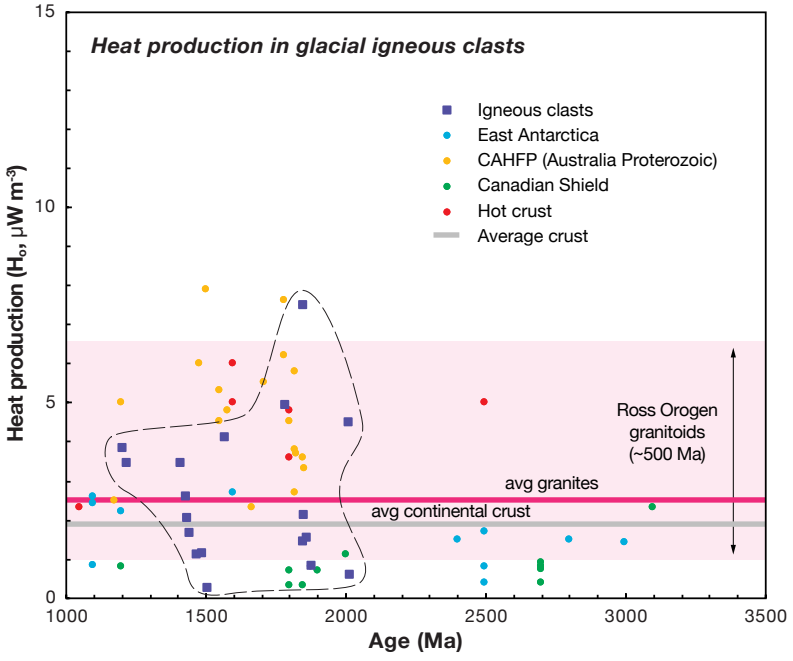


**Figure 3. Plot of surface heat production ($H_0$) vs. age for igneous glacial clasts. Data listed in Table 1. Range of heat production values in Ross Orogen granites from unpublished data. For comparison, values are shown from the Canadian Shield (Mareschal and Jaupart, 2013; Jaupart et al., 2016), areas of high heat production in stable continental provinces ('hot crust'; Mareschal and Jaupart, 2013; Jaupart et al., 2016), East Antarctica (Carson and Pittard, 2012; Carson et al., 2014), and the Central Australian Heat Flow Province (CAHFP; McLaren et al., 2003).**

The Cryosphere Discuss., https://doi.org/10.5194/tc-2017-134
Manuscript under review for journal The Cryosphere
Discussion started: 14 August 2017


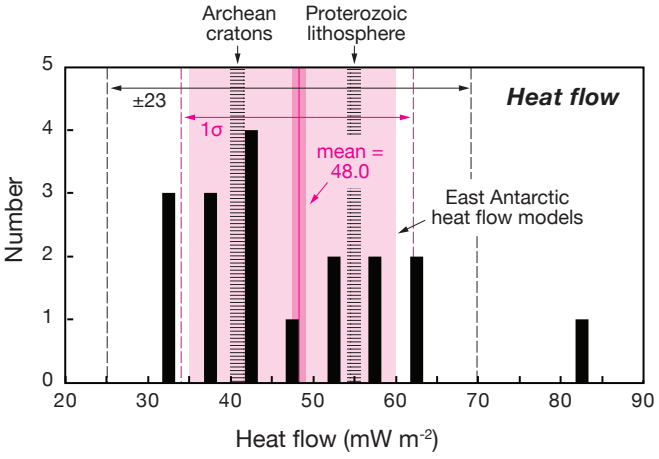


**Figure 4. Histogram of heat flow values estimated from heat production in the glacial clasts. Mean value (magenta) is 48.0 mW $m^{-2}$ (n = 18) with a 1σ standard deviation of 13.6 mW $m^{-2}$. Consideration of uncertainties in calculation of heat flow indicates an overall uncertainty of about ±21 mW $m^{-2}$ (see text). Range of heat flow modeled for East Antarctica shown for comparison (light pink, Van Liefferinge and Pattyn, 2013). Global average values for Archean cratons and Proterozoic lithosphere shown by ruled bars (Nyblade et al., 1999).**

The Cryosphere Discuss., https://doi.org/10.5194/tc-2017-134
Manuscript under review for journal The Cryosphere
Discussion started: 14 August 2017




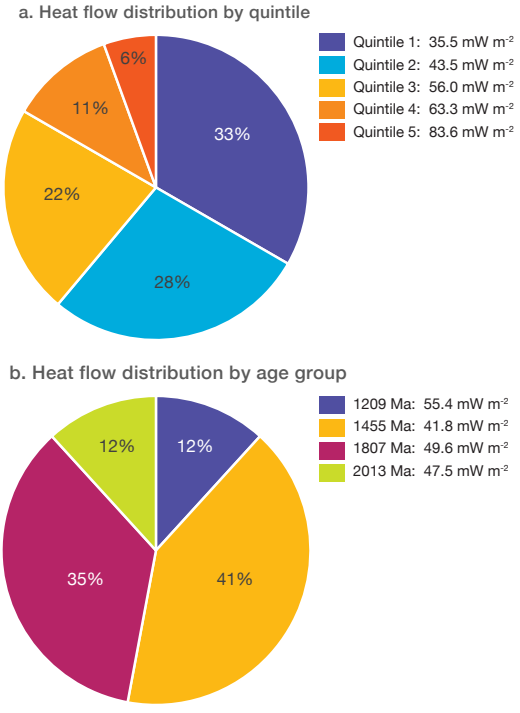


**Figure 5: Summary pie diagrams showing distribution of heat flow estimates from this study. (a) Distribution of heat flow by quintiles between 30-80 mW m$^{-2}$. Quintile averages shown, with the highest quintile represented by one sample with calculated heat flow of about 84 mW m$^{-2}$. (b) Distribution of average heat flow by age groups. Values shown in Table 2.**

5

The Cryosphere Discuss., https://doi.org/10.5194/tc-2017-134
Manuscript under review for journal The Cryosphere
Discussion started: 14 August 2017


**Table 1. Estimates of $H_o$ and $q_o$ for igneous clast samples, central East Antarctica.**

| Sample | Age (Ma) | U (ppm) | Th (ppm) | $K_2O$ (wt%) | $H_o$ (Method 1) [a] ($\mu W\ m^{-3}$) | $H_o$ (Method 2) [a] ($\mu W\ m^{-3}$) | $q_o$ [b] ($mW\ m^{-2}$) |
|---|---|---|---|---|---|---|---|
| 10LWA-13.1 | 1204 | 5.7 | 27.7 | 3.80 | 3.81 | 3.79 | 56.8 |
| 10LWA-11.1 | 1213 | 2.5 | 32.9 | 4.72 | 3.43 | 3.40 | 54.1 |
| 10MSA-2.3 | 1410 | 0.2 | 38.0 | 7.26 | 3.43 | 3.35 | 54.1 |
| 10TNA-1.1 | 1430 | 1.2 | 18.5 | 4.39 | 2.04 | 1.98 | 43.9 |
| 10LWA-6.5 | 1432 | 2.7 | 15.8 | 8.16 | 2.59 | 2.46 | 47.9 |
| 10LWB-4.3 | 1448 | 1.2 | 11.4 | 5.76 | 1.66 | 1.57 | 41.2 |
| 10LWB-3.8 | 1470 | 1.2 | 5.8 | 4.19 | 1.12 | 1.05 | 37.2 |
| 10LWA-20.1 | 1486 | 1.2 | 8.6 | 2.35 | 1.14 | 1.11 | 37.4 |
| 10MSA-3.5 | 1508 | n.d. | 1.5 | 1.57 | 0.25 | 0.23 | 30.9 |
| 10LWA-6.4 | 1570 | 6.4 | 26.9 | 5.65 | 4.11 | 4.05 | 59.0 |
| 10LWA-14.1 | 1786 | 5.4 | 41.9 | 5.77 | 4.93 | 4.89 | 65.0 |
| 10LWB-4.5 | 1848 | 0.5 | 13.4 | 3.89 | 1.45 | 1.39 | 39.6 |
| 10LWA-6.3 | 1850 | n.d. | 98.3 | 5.38 | 7.49 | 7.54 | 83.6 |
| 10LWA-7.1 | 1854 | 0.6 | 18.2 | 6.83 | 2.09 | 1.99 | 44.3 |
| 10LWB-4.1 | 1865 | 1.2 | 10.4 | 4.92 | 1.51 | 1.44 | 40.1 |
| 10MSA-3.3 | 1876 | 1.9 | 1.0 | 2.29 | 0.78 | 0.74 | 34.7 |
| 10LWA-10.1 | 2010 | 2.9 | 51.3 | 0.73 | 4.47 | 4.54 | 61.6 |
| 10LWA-8.1 | 2015 | 0.8 | 4.9 | 0.53 | 0.61 | 0.61 | 33.4 |
| Mean | | 2.0 | 23.7 | 4.34 | 2.61 | 2.56 | 48.0 |
| Std. dev. | | 2.0 | 24.0 | 2.18 | 1.86 | 1.89 | 13.6 |

[a] Heat production ($H_o$) was calculated from geochemical analysis in two ways. Method 1 uses Equation (1), using values after Rybach (1988) and Hasterok and Chapman (2011). Method 2 uses Equation (2). Both assume an average density ($\rho$) for granitic rocks of 2.7 x $10^3$ kg $m^{-3}$.

[b] Surface heat flow ($q_o$) determined from Equation (3) (Turcotte and Schubert, 2014).

**Table 2: Heat flow estimates in proportions based on quintile ranges and age.**

| Binned by quintile | | | | Binned by age | | | |
|---|---|---|---|---|---|---|---|
| Quintile | Heat flow ($mW\ m^{-2}$) | No. | % | Age (Ma) | Heat flow ($mW\ m^{-2}$) | No. | % |
| 1 | 35.5 | 6 | 0.33 | 1209 | 55.4 | 2 | 0.12 |
| 2 | 43.5 | 5 | 0.28 | 1455 | 41.8 | 7 | 0.41 |
| 3 | 56.0 | 4 | 0.22 | 1770 | 49.6 | 6 | 0.35 |
| 4 | 63.3 | 2 | 0.11 | 2013 | 47.5 | 2 | 0.12 |
| 5 | 83.6 | 1 | 0.06 | | | | |